Surface Functionalization of Porous Nanostructured Metal Oxide Thin Films Fabricated by Glancing Angle Deposition

Shufen Tsoi,[†] Enrico Fok,[‡] Jeremy C. Sit,*[,†] and Jonathan G. C. Veinot*[,‡]

Department of Electrical and Computer Engineering, University of Alberta, Edmonton, Alberta, T6G 2V4 Canada, and Department of Chemistry, University of Alberta, Edmonton, Alberta, T6G 2G2 Canada

Received July 21, 2006

We report the application of solution- and vapor-phase siloxane-based methods for tailoring the surface chemistry/properties of highly porous, nanostructured thin films fabricated using glancing angle deposition (GLAD). The GLAD technique produces high surface area films consisting of isolated columns and provides complete control over the film/column morphology. In the present study, the chemical tunability of a variety of metal oxide GLAD films was investigated using solution-based and vapor-phase surface functionalization methodologies. The surface properties and structures of the treated and untreated films were investigated using scanning electron microscopy (SEM), advancing aqueous contact angle measurements, cyclic voltammetry, and X-ray photoelectron spectroscopy (XPS). Results indicate that the surface chemistry of metal oxide GLAD films could be tailored by either method; however, chemical reactivity depends strongly on the metal oxide film material. Chemical tunability is demonstrated through the covalent tethering of numerous chemical moieties onto the exposed and interior surfaces of metal oxide GLAD films of varied structural motifs. Through careful choice of surface modifier, the present derivatization methods afford a full range of aqueous wettability from hydrophilic to superhydrophobic without compromising film structure. These functionalized, nanoconstructed films demonstrate a high degree of tunability over both structural and surface properties, making them well suited for diverse applications such as optical filters or sensors.

Introduction

High surface area, nanostructured materials have been studied extensively and have many potential applications including surface wetting/dewetting layers,[1−3] optical devices,[4−6] and sensors.[7−9] Surface chemistry and geometric structure can be exploited independently or in concert to control the wettability and chemical sensitivity of these functional materials.[1−3] Already, tailoring of surface chemistry and interfacial surface energy of indium tin oxide coatings has been shown to improve the performance metrics of organic light emitting diodes.[10−13] In a similar manner, optical bandpass filters whose response is dependent on relative humidity[14] and sensors that require high sensitivity and selectivity can also benefit from such an approach.[8]

Few examples combining tailored surface chemistry with well-defined, geometrically sculpted nanostructures exist; however, by simultaneous control of these properties, material surface wettability and chemical selectivity can be tuned without compromising other favorable material characteristics (e.g., surface area, optical response). Our group and others have demonstrated that highly porous, nanostructured thin films are conveniently fabricated using glancing angle deposition (GLAD).[4,5,14−16] The GLAD technique provides unprecedented structural and compositional control of micro/nanostructured films comprised of isolated semiordered columns. The column/pillar structure is readily sculpted into a variety of motifs through predictable variation of experimental conditions and nearly any solid compatible with physical vapor deposition techniques (thermal/electron-beam evaporation, sputtering, pulsed laser deposition) may be used.

* Authors to whom correspondence should be addressed. (J. Sit) Telephone: +1-780-492-3937; fax: +1-780-492-2863; e-mail: jsit@ece.ualberta.ca. (J. Veinot) Telephone: +1-780-492-7206; fax: +1-780-492-8231; e-mail: jveinot@ualberta.ca.

[†] Department of Electrical and Computer Engineering.

[‡] Department of Chemistry.

(1) Cheng, Y.-T.; Rodak, D. E. *Appl. Phys. Lett.* **2005**, *86*, 144101.
(2) Li, S.; Li, H.; Wang, X.; Song, Y.; Lui, Y.; Jiang, L.; Zhu, D. *J. Phys. Chem. B* **2002**, *106*, 9274.
(3) Sun, T.; Feng, L.; Gao, X.; Jiang, L. *Acc. Chem. Res.* **2005**, *38*, 644.
(4) van Popta, A. C.; Sit, J. C.; Brett, M. J. *J. Appl. Phys.* **2005**, *98*, 083517.
(5) van Popta, A. C.; Kennedy, S. R.; Broer, D. J.; Sit, J. C.; Brett, M. J. *Proc. SPIE* **2003**, *5213*, 232.
(6) Xue, J.; Rand, B. P.; Uchida, S.; Forrest, S. R. *Adv. Mater.* **2005**, *17*, 66.
(7) Virji, S.; Huang, J.; Kaner, R. B.; Weiller, B. H. *Nano Lett.* **2004**, *4*, 491.
(8) Steele, J. J.; Harris, K. D.; Brett, M. J. *Mater. Res. Soc. Symp. Proc.* **2004**, *788*, 473.
(9) Geobaldo, F.; Rivolo, P.; Ugliengo, P.; Garrone, E. *Sens. Actuators, B* **2004**, *100*, 29.
(10) Yan, H.; Huang, Q.; Cui, J.; Veinot, J. G. C.; Kern, M.; Marks, T. J. *Adv. Mater.* **2003**, *15*, 835.
(11) Cui, J.; Huang, Q.; Veinot, J. G. C.; Yan, H.; Marks, T. J. *Adv. Mater.* **2002**, *14*, 565.
(12) Cui, J.; Huang, Q.; Veinot, J. G. C.; Yan, H.; Wang, Q.; Hutchison, G. R.; Richter, A. G.; Evmenenko, G.; Dutta, P.; Marks, T. J. *Langmuir* **2002**, *18*, 9958.
(13) Malinsky, J. E.; Veinot, J. G. C.; Jabbour, G. E.; Shaheen, S. E.; Anderson, J. D.; Lee, P.; Richter, A. G.; Burin, A. L.; Ratner, M. A.; Marks, T. J.; Armstrong, N. R.; Kippelen, B.; Dutta, P.; Peyghambarian, N. *Chem. Mater.* **2002**, *14*, 3054.
(14) van Popta, A. C.; Hawkeye, M. M.; Sit, J. C.; Brett, M. J. *Opt. Lett.* **2004**, *29*, 2545.
(15) Robbie, K.; Friedrich, L. J.; Dew, S. K.; Smy, T.; Brett, M. J. *J. Vac. Sci. Technol., A* **1995**, *13*, 1032.
(16) Steele, J. J.; Gospodyn, J.; Sit, J. C.; Brett, M. J. *IEEE Sens. J.* **2005**, *6*, 24.

10.1021/cm061709t CCC: $33.50
Published on Web 10/10/2006

The semiordered structure and highly accessible surface area of GLAD films make them well-suited for optical,[5,14] sensing,[8,17−19] and catalytic[20] applications. The introduction of tailored surface chemistry to metal oxide GLAD-grown thin films will doubtless afford an effective avenue to realize sensitivity and selectivity needed if the latter of these applications are to be fully realized and optimized.

Glancing Angle Deposition. Traditional physical vapor deposition methods for solid thin film fabrication employ a source flux arriving normal to the substrate. During initial stages of film deposition, the impinging adsorbed atoms or adatoms condense on the substrate and diffuse within a limited range (dependent on thermal conditions) before settling into a local minimum low energy site, where they begin to form nuclei which have a material-dependent critical size for thermal stability. The nuclei continue to grow into larger clusters and eventually will coalesce to form a continuous film. Three parameters—surface diffusion, bulk diffusion, and atomic shadowing—govern structure and crystallinity of vapor-deposited thin films, as described in various structure-zone models (SZMs).[21,22] Both diffusion processes are thermal effects whose magnitudes depend on substrate temperature and deposition pressure. Atomic shadowing, on the other hand, depends on geometric factors arising from the three-dimensional nature of the nuclei. The Movchan and Dimchishin SZM proposes that films deposited onto heated substrates develop structures that exhibit a "Zone 2" smooth appearance with defected columnar grains created by surface diffusion or a "Zone 3" structure corresponding to annealed films with large grains and few defects.[22] The smooth appearance of films grown in these two regimes arises from surface diffusion while in the latter case bulk diffusion also plays a part. In contrast, when a thin film is deposited under conditions of low adatom mobility (e.g., a high melting point material deposited onto unheated substrates), "Zone 1" dome-shaped structures separated by void boundaries result. In this case, the diffusion effects are insufficient to overcome voiding arising from the atomic shadowing.

The atomic shadowing growth mechanism can be exploited and accentuated using the GLAD technique.[23,24] By holding the substrate at a glancing angle (α) measured from the normal of the substrate, growing nuclei present on the surface of the substrate create areas into which the obliquely arriving vapor flux cannot directly impinge. Deposition under conditions of limited adatom mobility (vide supra) and at high values of α accentuates the shadowing mechanism, creating void areas in the film that are not filled, and a high porosity, high surface area thin film of isolated columnar structures forms. Holding the substrate fixed at an extreme oblique angle (typically 75−85°) during deposition produces a slanted post thin film, the simplest fundamental GLAD film archetype. Because film growth tends toward the incoming vapor flux, the morphology of the film can be tuned in situ using the GLAD apparatus that affords high-resolution control of both the polar (α) and azimuthal (φ) directions from which the source flux arrives at the substrate. Systematic variation of the speed and direction of rotation about these two axes leads to the growth of numerous pillar and graded-index structures. Helical GLAD films are realized by continuously "steering" the film growth direction via slow, constant (relative to the deposition rate) substrate rotation in φ. If the rotation rate is sufficiently rapid, helices degenerate into vertical cylindrical posts. Other structures such as chevron or "square spiral" nanostructures are formed through stepped rotation in φ.[14,25−27] The high porosity and surface area, as well as material and structure versatility, of GLAD films have lead to many applications including sensing,[18−20] photonic band gaps (PGB),[26−28] optical devices,[14,29] and broad-band antireflection coatings.[30] One particularly intriguing example that interfaces GLAD films with functional organic molecules involves filling hydrophilic, helical structured SiO_2 or TiO_2 GLAD films with known, hydrophobic liquid crystals to enhance the chiral optical response.[5,31] Periodic square spirals fabricated using the GLAD method have been demonstrated as a promising approach to the fabrication of 3-D photonic band gap crystals; however, their properties are influenced by environmental conditions (e.g., humidity).[26,27,32] High-speed humidity sensors exploiting the sensitivity of the electrical capacitance of vertical post GLAD films have also been demonstrated by Steele et al.[8] Clearly, many of the current and future applications of GLAD films require interfacing functional, hydrophobic or hydrophilic chemical species with hydrophilic structures. If those device applications that are susceptible to environmental conditions or that exploit the combined properties from interfaced hydrophilic nanostructured films and hydrophobic organic materials are to be realized, methods for controlling the surface energy of GLAD films must be developed.

In short, two properties influence the surface hydrophobicity of a material: structure (e.g., roughness) and chemistry. It has been demonstrated that GLAD film hydrophobicity can be tailored through systematic aspect ratio variation.[33] Still, only limited control over interaction with aqueous solvents can be achieved by varying film thickness or pillar density as this approach provides no control over the chemical response of the GLAD films.

(17) Harris, K. D.; Vick, D.; Gonzalez, E. J.; Smy, T.; Robbie, K.; Brett, M. J. *Surf. Coat. Technol.* **2001**, *138*, 185.
(18) Harris, K. D.; Huizinga, A.; Brett, M. J. *Electrochem. Solid−State Lett.* **2002**, *5*, H27.
(19) Wu, A. T.; Brett, M. J. *Sens. Mater.* **2001**, *13*, 399.
(20) Harris, K. D.; McBride, J. R.; Nietering, K. E.; Brett, M. J. *Sens. Mater.* **2001**, *13*, 225.
(21) Thornton, J. A. *Annu. Rev. Mater. Sci.* **1977**, *7*, 239.
(22) Movchan, A.; Demchishin, A. V. *Phys. Met. Metallogr.* **1969**, *28*, 83.
(23) Vick, D.; Friedrich, L. J.; Dew, S. K.; Brett, M. J.; Robbie, K.; Seto, M.; Smy, T. *Thin Solid Films* **1999**, *339*, 88.
(24) Robbie, K.; Brett, M. J. *J. Vac. Sci. Technol., A* **1997**, *15*, 1460.
(25) Seto, M.; Westra, K.; Brett, M. J. *J. Mater. Chem.* **2002**, *12*, 2348.
(26) Kennedy, S. R.; Brett, M. J.; Miguez, H.; Toarder, O.; John, S. *Photon. Nanostruct.- Fundam. Appl.* **2003**, *1*, 37.
(27) Jensen, M. O.; Kennedy, S. R.; Brett, M. J. *Mater. Res. Soc. Symp. Proc.* **2002**, *728*, 203.
(28) Summers, M. A.; Kennedy, S. R.; Elias, A.; Jensen, M. O.; Harris, K. D.; Szeto, B.; Brett, M. J. *Proc. SPIE* **2004**, *5347*, 170.
(29) Hrudey, P. C. P.; Taschuk, M.; Tsui, Y. Y.; Fedosejevs, R.; Sit, J. C.; Brett, M. J. *J. Nanosci. Nanotechnol.* **2005**, *5*, 1.
(30) Kennedy, S. R.; Brett, M. J. *Appl. Opt.* **2003**, *42*, 4573.
(31) van Popta, A. C.; Sit, J. C.; Brett, M. J. *Appl. Opt.* **2004**, *43*, 3632.
(32) Kennedy, S. R.; Brett, M. J. *J. Vac. Sci. Technol., B* **2004**, *22*, 1184.
(33) Fan, J. G.; Tang, X. J.; Zhao, Y. P. *Nanotechology* **2004**, *15*, 501.

Siloxane-based surface chemistry is a well-established method for controlling the surface properties of a variety of substrates (e.g., crystalline silicon, glass, ITO). The versatility and durability of siloxane-grafted molecular films are well illustrated by works using these robust surface moieties for nanolithography,[34−38] microcontact printing,[39,40] ordering metal nanoparticles,[41] and enhancing the performance of opotoelectronic devices.[10,12,42−46] Previously, we demonstrated in proof-of-concept work that a straightforward, solution-based self-assembly method employing commercially available reagents and SiO_2 GLAD films exploited the synergistic effects of film morphology and tailored surface chemistry to yield hydrophobic and superhydrophobic surfaces.[38]

In this study, we widen the scope of study to additional functionalization methods of GLAD thin films of a range of metal oxides important for applications in sensors and optical devices. We outline here three independent, straightforward, siloxane-based methods (including solution-based and vapor-phase procedures) while describing influences on surface wettability because of the underlying film material (SiO_2, TiO_2, and Al_2O_3), the GLAD film structural motif, and the surface modifier chemical structure.

Experimental

Materials and Methods. Borofloat glass and indium tin oxide (ITO)-coated borofloat glass (rms roughness = 2.17 nm over an area of 5 μm^2, measured using atomic force microscopy) were supplied by Precision Glass & Optics and were used as received. *n*-Type silicon {100} wafers were supplied by Evergreen Semiconductor Materials. Si wafers were cleaned by immersing in piranha solution (3:1 vol % H_2SO_4:H_2O_2) for 30 min followed by rinsing with deionized water and drying in a flow of nitrogen. Evaporant source materials (TiO_2, SiO_2, and Al_2O_3) were obtained as 99% purity 3−6 mm pieces and were used as received from CERAC, Inc. Octadecyl-trichlorosilane, vinyl-trichlorosilane, 3,3,3-trifluoropropyl-trichlorosilane, and 7-octen-1-yl-trimethoxysilane were used as received from Aldrich Chemical Co. Reagent-grade acetone and toluene were supplied by Fisher Scientific. Dry, deoxygenated toluene was obtained by distilling over sodium/benzophenone under Ar atmosphere and was used immediately.

Scanning electron microscopy (SEM) imaging of films before and after chemical functionalization was perfomed using a JEOL 6301F field-emission scanning electron microscope with an acceleration voltage of 5 kV. Advancing aqueous contact angles were measured on a First Ten Angstroms FTA100 Series contact angle/surface energy analysis system using deionized water as the probe liquid.

Glancing Angle Deposition. TiO_2, SiO_2, and Al_2O_3 GLAD films of slanted posts, vertical posts, and helical columnar structure used in the present study were fabricated using procedures detailed in the literature.[15,24,47,48] In brief, metal oxide source pellets were placed in 8.2 cm^3 carbon crucibles supplied by POCO Graphite and were evaporated using electron-beam evaporation. The in-situ deposition rate and film thickness were tracked using a standard cystal oscillator thickness/rate monitor utilizing 6 MHz quartz/alloy crystals supplied by Phelps Electronics, Inc. Films (ca. 2.0-μm thick) were deposited onto various substrates listed above at glancing angle $\alpha = 85°$. For slanted posts, the substrate was maintained at constant α with no rotation about the φ axis. Uniform helical structures were fabricated with φ rotation of 0.21 rpm, while maintaining a deposition rate at 14 Å/s. Films with vertical post morphology were grown with φ rotation of ∼17 rpm while maintaining the deposition rate at 18 Å/s. For the present study, SiO_2 films were deposited at a vacuum base pressure below 5×10^{-6} Torr (7×10^{-4} Pa), while TiO_2 and Al_2O_3 films were deposited at vacuum base pressures below 2×10^{-7} Torr (3×10^{-5} Pa).

Reactive Ion Etching. All film samples were treated with oxygen plasma reactive ion etching (RIE) using a Plasmalab RIE80 to saturate the film surface with hydrophilic hydroxyl (−OH) groups prior to surface functionalization. Prior to O_2 plasma treatment, the RIE system chamber was purged for 30 min using 80% of 100 sccm O_2 flow and 75% of 350 W radio frequency (RF) power. Following this cleaning protocol, all GLAD films were treated with O_2 plasma using the same procedure but limited to 90 s.

Solution-Based Alkyl Siloxane Surface Functionalization. Following Schlenk protocol, ITO-coated borofloat glass, uncoated glass, and Si{100} substrates with and without metal oxide GLAD films (SiO_2, TiO_2, Al_2O_3) were fully immersed in a dry, deoxygenated 20 mM toluene solution of alkyltrichlorosilane (octadecyl-trichlorosilane, vinyl-trichlorosilane, 3,3,3-trifluoropropyl trichlorosilane, or 7-octen-1-yl-trimethoxysilane) and were allowed to react for 24 h under argon atmosphere. The solution was removed then by cannula and the samples were rinsed three times with dry toluene then were immersed in acetone (ca. 5% H_2O) to hydrolyze any residual Si−Cl functionalities and were finally annealed in air for 24 h at 150 °C.[13]

Vapor-Phase Surface Functionalization. Substrates with and without metal oxide GLAD films were placed inside a vacuum desiccator containing an open glass vial with 1.0 mL of appropriate alkyltrichlorosilane (7-octen-1-yl-trimethoxysilane, 3,3,3-trifluoropropyl-trichlorosilane). Substrates were reacted for 48 h under static-reduced pressure in a saturated atmosphere of the organosilane.

X-ray Photoelectron Spectroscopy (XPS). A Kratos Axis Ultra instrument operating in energy spectrum mode at 210 W was used for XPS measurements. The base pressure and operating chamber pressure was maintained at $\leq 10^{-7}$ Pa. A monochromatic Al K-α source was used to irradiate the samples, and the spectra were obtained with an electron takeoff angle of 90°. Wide survey spectra were collected using an elliptical spot with 2 mm and 1 mm major and minor axis length, respectively, and 160 eV passing energy with a step of 0.33 eV. Film compositions were determined from the peaks of the survey spectra with subtracted linear background using the internal instrument values of relative sensitivity factor.

(34) Maoz, R.; Frydman, E.; Cohen, S. R.; Sagiv, J. *Adv. Mater.* **2000**, *12*, 725.
(35) Maoz, R.; Frydman, E.; Cohen, S. R.; Sagiv, J. *Adv. Mater.* **2000**, *12*, 424.
(36) Liu, S.; Maoz, R.; Schmid, G.; Sagiv, J. *Nano Lett.* **2002**, *2*, 1055.
(37) Hoeppener, S.; Maoz, R.; Sagiv, J. *Nano Lett.* **2003**, *3*, 761.
(38) Tsoi, S.; Fok, E.; Sit, J. C.; Veinot, J. G. C. *Langmuir* **2004**, *20*, 10771.
(39) St. John, P. M.; Craighead, H. G. *Appl. Phys. Lett.* **1995**, *68*, 1022.
(40) Xia, Y.; Mrksich, M.; Kim, E.; Whitesides, G. M. *J. Am. Chem. Soc.* **1995**, *117*, 9576.
(41) Hoeppener, S.; Maoz, R.; Cohen, S. R.; Chi, L.; Fuchs, H.; Sagiv, J. *Adv. Mater.* **2002**, *14*, 1036.
(42) Huang, Q.; Cui, J.; Veinot, J. G. C.; Yan, H.; Marks, T. J. *Appl. Phys. Lett.* **2003**, *82*, 331.
(43) Faccheti, A.; Abbotto, A.; Beverina, L.; van der Boom, M. E.; Dutta, P.; Evmenenko, G.; Pagani, G. A.; Marks, T. J. *Chem. Mater.* **2003**, *15*, 33.
(44) Huang, Q.; Kang, H.; Veinot, J.; Yan, H.; Zhu, P.; Marks, T. J. In *Organic Nanophotonics*; Agranovich, V., Charra, F., Kajzar, F., Eds; Kluwer Publishers: Dordrecht, The Netherlands, 2003; p 241.
(45) Wang, G.; Zhu, P.; Marks, T. J.; Ketterson, J. B. *Appl. Phys. Lett.* **2002**, *81*, 2169.
(46) Zhu, P.; van der Boom, M. E.; Kang, H.; Evmenenko, G.; Dutta, P.; Marks, T. J. *Chem. Mater.* **2002**, *14*, 4982.
(47) Robbie, K.; Shafai, C.; Brett, M. J. *J. Mater Res* **1999**, *14*, 3158.
(48) Robbie, K.; Brett, M. J. *J. Vac. Sci. Technol., A* **1995**, *13*, 2991.

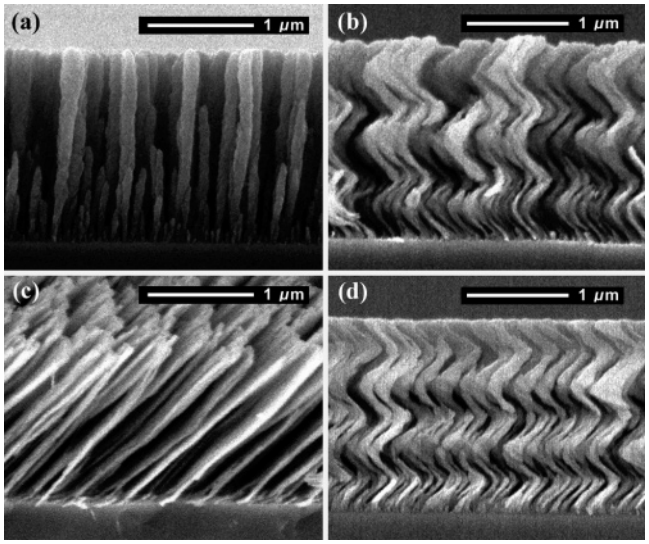

Figure 1. SEM images of SiO_2 GLAD films of varied structural motifs: (a) vertical posts, (b) helices, (c) slanted posts, and (d) helices after solution-based functionalization with octadecyl-trichlorosilane. Similar images were observed for the various SiO_2 nanostructures following RIE treatment.

Results and Discussion

SiO_2, Al_2O_3, and TiO_2 GLAD structures with a variety of morphologies (slanted posts, vertical posts, and helices) were deposited onto numerous substrates (Si{100} wafers, borofloat glass, ITO-coated borofloat glass) (Figure 1). All films prepared for this study show the well-defined columnar structure and high surface area characteristic of films previously prepared using the GLAD technique. To facilitate effective reaction with organotrichloro- and trimethoxysilane reagents, all samples were exposed to oxygen plasma reactive ion etching to render the surface hydrophilic and to saturate it with hydroxyl moieties.[13] Scanning electron micrographs show no detectable damage to film structure arising from the RIE procedure.

Solution-Based Organotrichlorosilane Surface Functionalization. The surfaces of oxygen plasma RIE-treated slanted, vertical, and helical structured posts of SiO_2, Al_2O_3, and TiO_2 films on Si{100}, borofloat glass, and ITO-coated borofloat glass substrates are susceptible to solution reaction with vinyl-trichlorosilane and 3,3,3-trifluoropropyl-trichlorosilane. Exposure to 20 mM toluene solutions of organotrichlorosilane reagents at room temperature affords effective surface functionalization with no obvious degradation to any presented metal oxide pillars as evidenced by close examination of the helical fine structure using SEM (Figure 1d).

Similar alkyl trichlorosilane-based self-assembly procedures have been used to tailor the surface chemistry of conductive indium tin oxide (ITO).[49] Insight into surface modification process was obtained when GLAD films deposited on conducting ITO substrates were examined. XPS spectra of bare ITO-coated glass, surface-functionalized ITO, as well as as-deposited and functionalized SiO_2 GLAD films on ITO show changes readily attributed to surface chemistry arising from the derivatization procedure.[37] The present organotrichlorosilane solution functionalization procedure presented for SiO_2 GLAD films is readily transferable to

(49) Choi, B.; Rhee, J.; Lee, H. H. *Appl. Phys. Lett.* **2001**, *79*, 2109.

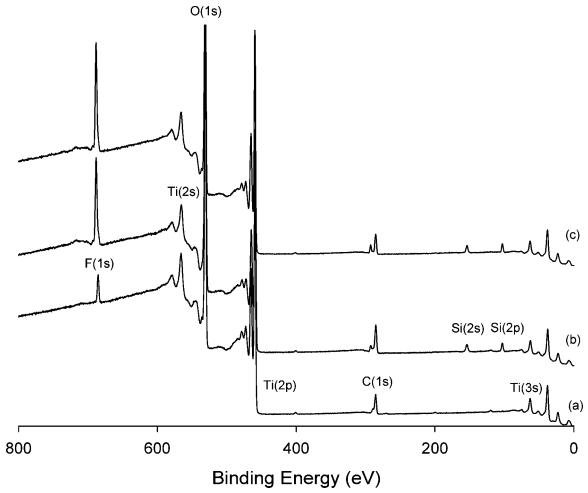

Figure 2. XPS results for helical TiO_2 GLAD films on Si{100}: (a) as-deposited film; 3,3,3-trifluoropropyl-trichlorosilane-derivatized film by (b) solution-based method and (c) vapor-phase method.

Al_2O_3 and TiO_2 GLAD systems. XPS analyses of these functionalized samples show decreases in emissions arising from the GLAD pillars (i.e., Al(2s), Al(2p) and Ti(2s), Ti-(2p)) and the increase/appearance of emissions arising from the surface-bonded functionality (e.g., C(1s), Si(2s), and Si-(2p)) (Figures 2b and 3b). This observed increase of C(1s) and appearance of Si(2s) and Si(2p) signals from the functionalized TiO_2 and Al_2O_3 films support a change in GLAD film surface chemistry consistent with the attachment of the organic moieties. In addition, the full hydrolysis of Si−Cl bonds and complete removal of any residual HCl byproducts during the solution-based derivatization process on metal oxide GLAD pillars has been confirmed to sensitivity level afforded by XPS given the absence of Cl-(2p) emission. Similar results were noted for GLAD samples prepared on borofloat glass substrates.

To investigate whether solution-borne trichlorosilane reagents penetrate into high surface area GLAD structures and react with the underlying substrate, cyclic voltammetry was performed. A typical experiment used a GLAD film on ITO with or without functionalization as the working electrode. The well-characterized, reversible ferrocene/ferrocenium redox process was employed as an electrochemical probe with bare ITO, functionalized ITO, neat GLAD films on ITO, and functionalized GLAD films on ITO as working electrodes. When unfunctionalized ITO-coated glass substrates with or without GLAD films were used as the working electrode, the reversible ferrocene/ferrocenium redox couple is observed. Upon derivatization with vinylsiloxane, the reversible Fe^{2+}/Fe^{3+} redox process is replaced by an irreversible oxidation process.[37] This is directly analogous to that seen for ITO electrodes functionalized with an electroactive vinylsiloxane molecular layer and indicates that the vinyl-trichlorosilane penetrates effectively into the GLAD structure to chemically modify the underlying substrate. Hence, it is reasonable to expect that the interior pillar surfaces are also modified.

An important observation of the present studies highlighting the sensitivity of GLAD films to trace reaction impurities arises when freshly distilled solvents are not used in the surface functionalization procedure. We have noted that, in

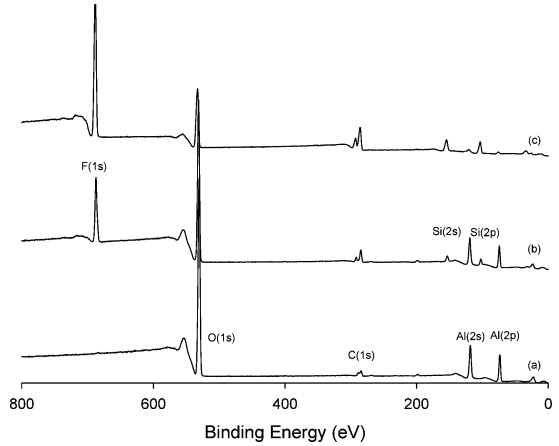

Figure 3. XPS results for helical Al_2O_3 GLAD films on Si{100}: (a) as-deposited film; 3,3,3-trifluoropropyl-trichlorosilane-derivatized film by (b) solution-based method and (c) vapor-phase method.

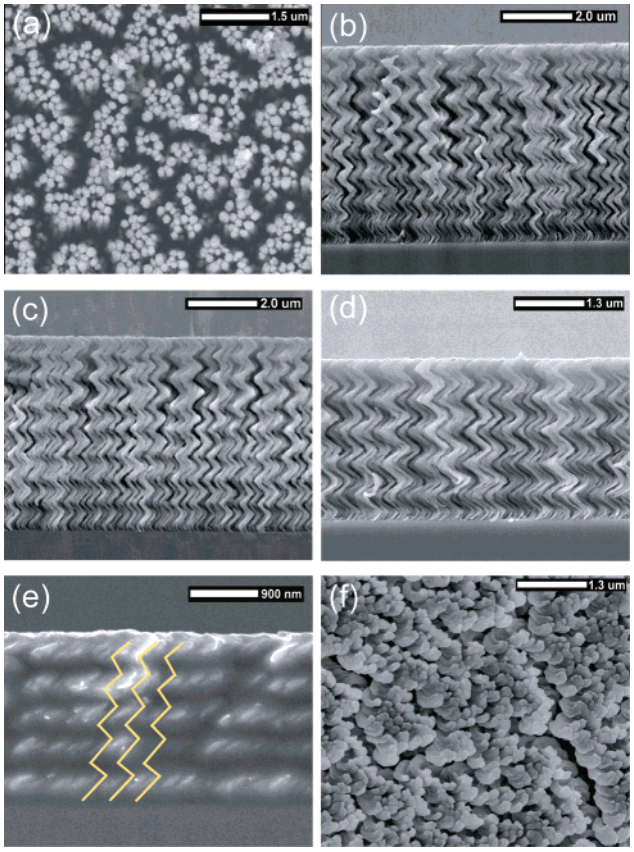

Figure 4. Top view SEM image of (a) solution-based vinyl-trichlorosilane-derivatized SiO_2 GLAD film showing clumped columns because of trace water impurities present in reactant solution. Representative edge view SEM images of various 3,3,3-trifluoropropyl-tricholorosilane-derivatized GLAD films: (b) solution-derivatized SiO_2 film; (c) vapor-phase-derivatized TiO_2 film; (d) solution-derivatized Al_2O_3; (e) vapor-phase-derivatized Al_2O_3 showing film interstices filled because of undesired side reaction (the lines highlight the remaining traces of the original helical structure). (f) A top view of e.

the presence of trace water impurities, the GLAD pillars tend to agglomerate into "haystack"-like structures (Figure 4a). Our observations are similar to, however less pronounced than, the "nanocarpet effect" reported by Fan et al.[50] and attributed to the effects of capillary action. The formation of these haystacks and loss of regular film structure could hinder many device applications relying on this property of GLAD films.

Vapor-Phase Organotrichlorosilane Surface Functionalization. To minimize pillar agglomeration and solvent waste and to demonstrate flexibility in our approach for tailoring of GLAD film surface properties, we have extended our studies to include vapor-phase functionalization of SiO_2, Al_2O_3, and TiO_2 films. The surface properties of SiO_2, TiO_2, and Al_2O_3 helical GLAD films on Si{100} and glass substrates were tailored using vapor-phase functionalization methods. Films were placed in a vacuum desiccator with an open vial containing 1 mL of the desired, volatile organotrichlorosilane. The desiccator was evacuated and filled with reagent vapor, and the substrates were exposed for 48 h.

As expected, SEM micrographs of vapor-phase surface-functionalized SiO_2 and TiO_2 films show unchanged film microstructure and no agglomeration (Figure 4b, c). In stark contrast, SEM images of vapor-phase treated helical Al_2O_3 films, while still showing some evidence of the underlying film nanostructure, indicate that the film void volume was almost completely filled (Figure 4e, f) and that the pillars had increased in diameter. This observation is understood in the context of well-established reactivities of SiO_2, TiO_2, and Al_2O_3 with HCl. Specifically, SiO_2 and TiO_2 are known to be resistant to HCl whereas Al_2O_3 neutralizes it. This alone makes Al_2O_3 GLAD structures more susceptible to degradation under organotrichlorosilane reaction conditions. Unfortunately, the elimination of HCl from the present reaction is nontrivial. There are several sources of HCl including the byproduct of the organotrichlorosilane surface reaction, impurities in the as-received organosilane reagents, and trace amounts of water vapor in the desiccator that could hydrolyze some of the trichlorosilane reagent producing HCl. Regardless of the source of HCl, its presence causes deterioration of the alumina film and further underscores the importance of alternative functionalization methodologies presented here. It is reasonable that aluminum oxide GLAD films react with HCl to yield complex aluminum chlorides that react in ambient conditions to yield hydrated alumina.[51] This reaction would result in GLAD pillars expanding to fill the film void volume. While it is unfortunate that this side reaction leads to permanent destruction of Al_2O_3 films, it does support our electrochemical observations that siloxane functionalization proceeds to the underlying substrate surface (vide supra). Clearly, SEM images show the Al_2O_3 GLAD structures broaden uniformly as a result of this reaction. Similar pillar broadening was not observed for the solution functionalization of Al_2O_3 because of reduced activity of HCl in organic media.

XPS analysis of vapor-functionalized TiO_2 and SiO_2 GLAD films shows emissions arising from the surface modification that are more intense than the same signals noted for analogous solution derivatized samples, suggesting the vapor-phase surface functionalization is more efficient than the solution process. Unmodified TiO_2 GLAD films (Figure 2a) present characteristic Ti(2s), Ti(2p), Ti(3s), and O(1s) signals and a C(1s) emission that can be attributed to

(50) Fan, J. G.; Dyer, D.; Zhang, G.; Zhao, Y.-P. *Nano Lett.* **2004**, *4*, 2133.

(51) Thompson, W. R.; Pemberton, J. E. *Langmuir* **1995**, *11*, 1.

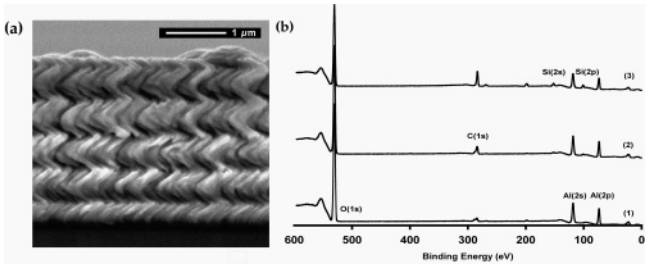

Figure 5. (a) SEM image of 7-octeny-1-yl-trimethoxysilane vapor-phase-functionalized Al_2O_3 helices. Similar images were observed for untreated and solution-functionalized Al_2O_3 helices. (b) XPS results for (1) untreated film; film functionalized with 7-octeny-1-yl-trimethoxysilane by (2) solution-phase and (3) vapor-phase methods.

trace carbon impurities that are omnipresent in the XPS analysis chamber. Following vapor-phase functionalization with 3,3,3-trifluoropropyl-trichlorosilane, slight decreases in the emission intensity arising from the GLAD pillars, a noticeable increase in C(1s), and the appearances of Si(2s), Si(2p), and F(1s) emissions were observed (Figure 2c). Similar results were noted for SiO_2 films. In contrast, a large decrease in all emissions associated with the GLAD film is observed from the vapor-phase functionalized Al_2O_3 spectra (Figure 3c) with respect to the untreated Al_2O_3 control sample. Yet, the F(1s) and C(1s) emission from the vapor-phase treated Al_2O_3 film was substantially higher than the untreated or solution-treated Al_2O_3 film. This is consistent with our proposal that Al_2O_3 has reacted with HCl, and hence we do not see the strong characteristic signals from Al_2O_3 film. Furthermore, the noted decrease of Al(2s), Al(2p), and O(1s) emissions confirms a decrease in the mass concentration of Al and O at the surface which leads to an increase in mass concentration of F and C in the aluminum oxide film.

Organotrimethoxysilane GLAD Film Surface Functionalization. To eliminate the detrimental side reaction of HCl with Al_2O_3 GLAD films, we have investigated GLAD film surface functionalization with organotrimethoxysilanes, reagents previously used to functionalize solid Al_2O_3 thin films[52] and beads[53] via solution-based methods. While alkyltrimethoxysilanes are known to react more slowly than alkyltrichlorosilanes,[54] from our observations, this does not hinder Al_2O_3 GLAD film surface modification, and the methanol reaction byproduct does not degrade the film. Using the same solution-based and vapor-phase procedures described herein for alkyltrichlorosilanes, SiO_2, TiO_2, and Al_2O_3 GLAD films were surface-functionalized with 7-octen-1-yl-trimethoxysilane. SEM indicates no significant changes in film microstructure upon exposure to organotrimethoxysilanes (Figure 5a). Consistent with our observations for relative XPS emission intensity of GLAD surfaces modified with organotrichlorosilanes, Figure 5b shows more pronounced Si(2s) and Si(2p) emissions for vapor organomethoxysilane functionalized films. In addition, XPS analysis of all films derivatized using solution- and vapor-phase protocols with 7-octen-1-yl-trimethoxysilane show an

(52) Jeon, N. L.; Finnie, K.; Branshaw, K.; Nuzzo, R. G. *Langmuir* **1997**, *13*, 3382.
(53) Visintin, P. M.; Carbonell, R. G.; Schauer, C. K.; DeSimone, J. M. *Langmuir* **2005**, *21*, 4816.
(54) Kallury, K. M. R.; Krull, U. J.; Thompson, M. *Org. Mass Spectrom.* **1991**, *26*, 81.

Table 1. Contact Angle Measurements of Untreated, O_2 Plasma Reactive Ion Etch (RIE) Treated, and Solution-Functionalized ITO Substrates and Nanostructured SiO_2 GLAD Films

		SiO_2		
treatment	ITO	vertical posts	slanted posts	helices
untreated	85°	0°	0°	0°
RIE-treated	0°	0°	0°	0°
vinyl-trichlorosilane	111°	128°	124°	122°
octadecyl-trichlorosilane	N/A	129°	126°	124°

expected increase in C(1s) and, for TiO_2 and Al_2O_3 films, appearance of Si(2s), Si(2p) supporting a surface siloxane linkage. However, when functionalized in solution, the intensity of Si(2s) and Si(2p) emissions noted for alkyltrimethoxysilane-derivatized Al_2O_3 are significantly lower than those of equivalent alkyltrichlorosilane-derivatized Al_2O_3 films. Doubtless, this arises from the well-established relative reactivities of the two reagents.[54]

Surface Functionalization Induced Hydrophobicity. One physical manifestation of GLAD surface functionalization is tailoring of hydrophobicity. The advancing aqueous contact angle (CA) of as-received bare ITO-glass substrates was found to be $\theta = 85°$ (Table 1). After short RIE treatment, the bare ITO surface becomes hydrophillic (i.e., $\theta = 0°$), consistent with a surface saturated with hydroxyl groups.[13] Upon functionalization with alkyl- and alkenyltrichlorosilanes, we note that the ITO-glass substrate exhibits a contact angle of $\theta = 111°$ (Table 1), demonstrating an increase in the hydrophobicity of the ITO surface.

As-prepared GLAD films exhibit an advancing aqueous contact angle of 0°, independent of the pillar structure, material, or underlying substrate. It is unclear if this surface property is the result of the GLAD porous structure, film surface chemistry, or—more probably—a combination of the two. Following surface derivitization with alkyltrichlorosilanes, the surfaces of present SiO_2 GLAD structures exhibit differing degrees of hydrophobicity. It is clear that the introduction of GLAD films causes a significant increase in CA (e.g., for ITO-coated glass samples functionalized with octadecyl-trichlorosilane: with a SiO_2 GLAD film, $\theta = 127°$, but with no GLAD film, $\theta = 111°$). A comparison of CAs for alkyl- and alkenyl-functionalized GLAD films of varied structural motifs reveals a trend $\theta_{\text{pillars}} > \theta_{\text{slanted post}} > \theta_{\text{helices}}$ (Table 1). Unfortunately, this trend is inconclusive because of the uncertainty of CA measurements. This is not the case for fluorinated surface modifiers (e.g., $R = -CH_2CH_2CF_3$) for which pillars exhibit significantly greater hydrophobicity than helices as illustrated through a comparison of Figure 6b and 6c (i.e., $\theta_{\text{pillars}} > 150°$, $\theta_{\text{helicies}} = 120°$). From straightforward geometrical considerations, it can be seen that helices have greater contact area with the water droplet than equivalent pillars (Figure 7). This increase in contact area decreases the hydrophobicity of the rough film surface as described by the modified Cassie and Baxter equation:[55]

$$\cos \theta' = f \cos \theta - (1 - f) \qquad (1)$$

where θ' is the apparent contact angle on a rough surface, θ is the intrinsic CA on a flat surface, f is the fraction of the

(55) Cassie, A. B. D.; Baxter, S. *Trans. Faraday Soc.* **1944**, *40*, 546.

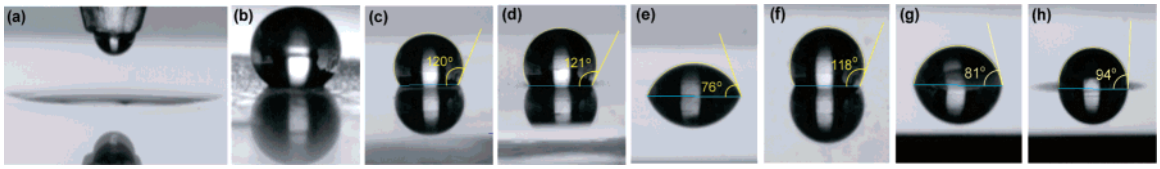

Figure 6. Representative aqueous advancing contact angle measurements of (a) nontreated and oxygen-RIE-treated SiO_2, TiO_2, Al_2O_3 GLAD films; various 3,3,3-trifluoropropyl-trichlorosilane-derivatized GLAD films: (b) solution-derivatized vertical post SiO_2; (c) solution- and (d) vapor-phase-derivatized helical SiO_2; (e) solution- and (f) vapor-phase-derivatized helical TiO_2; (g) solution- and (h) vapor-phase-derivatized helical Al_2O_3. All presented films were deposited on Si{100}.

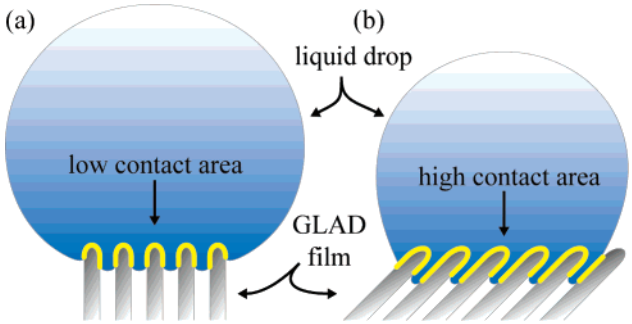

Figure 7. Schematic representation showing reduced contact areas for the liquid drop on (a) vertical posts as compared to (b) slanted posts or helices. The reduced contact area leads to higher apparent contact angles measured for case a.

solid/water interface, and $(1 - f)$ is the fraction of air/water interface. Clearly, the greater the solid/water contact, the smaller CA becomes.

The chemical structure of the surface modifier also clearly influences the hydrophobicity of functionalized GLAD films. This dependency is well illustrated by the trend of advancing aqueous contact angles for SiO_2 GLAD pillars bearing $R = -OH$, $-CH{=}CH_2$, $-CH_2(CH_2)_{16}CH_3$, and $-CH_2CH_2CF_3$ for which CAs lie in the range from 0° to 128°. As expected, hydroxyl moieties render the surface hydrophilic, simple hydrocarbon chains render surface hydrophobic, and fluorinated surface modifiers result in superhydrophobicity.

The vapor- and solution-phase functionalization of helical SiO_2 GLAD films produce nearly identical advancing aqueous CAs (e.g., for $R = -CH_2CH_2CF_3$, $\theta = 120°$ and 121° for solution-based and vapor-phase treatments, respectively); however, this is not the case for analogous Al_2O_3 and TiO_2 structures. For Al_2O_3 films derivitized with the fluorinated surface modifier, solution-based treatment resulted in $\theta = 81°$ while vapor-phase dervitization resulted in destruction of the film as described earlier. For the TiO_2 films treated with 3,3,3-trifluoropropyltrichlorosilane, $\theta_{solution} = 76°$ and $\theta_{vapor} = 118°$. The present CA measurement for TiO_2 is similar to that reported by Advincula et al. for solution-based functionalization of high surface area sol−gel derived TiO_2.[56] The lower contact angle for solution-functionalized Al_2O_3 and TiO_2 compared to analogous SiO_2 films arises from the relative reactivities of the metal oxides. It is currently unclear why solution-functionalized TiO_2 GLAD films are less hydrophobic than their vapor-phase-derivatized counterparts, however, a qualitative comparison of the relative intensities of Si(2s) and Si(2p) XPS emissions of vapor- and solution-derivatized films suggests a greater Si concentration at the surface of the vapor-treated GLAD. While the present data is not conclusive, it does suggest more efficient surface functionalization results from vapor derivatization. Yet another, equally plausible explanation may be the greater accessibility of GLAD film internal structure to vapor functionalization. The precise explanation for the difference in contact angles measured on vapor-phase and solution-treated TiO_2 film is currently under investigation.

(56) Advincula, M.; Fan, X.; Lemons, J.; Advincula, R. *Colloids Surf., B* **2005**, *42*, 29.

Conclusions

We have demonstrated both solution- and vapor-phase surface functionalization as effective methodologies for tethering various chemical moieties to the surface of complex, nanostructured, porous thin films fabricated by glancing angle deposition. XPS and electrochemistry support changes in the surface chemistry of all treated samples. The combination of the porous, columnar nature of GLAD film morphologies with surface chemistry modification leads to synergistic effects on film wettability. Clearly, both film structure and surface chemistry have strong influence on surface hydrophobicity as evidenced by advancing aqueous contact angle measurements. SEM imaging showed that, in general, the film structure is unaffected by the functionlization process. However, trace water impurities in the solvents used in the solution-based method caused film columns to "clump" together. Also, for the vapor-phase method, the reactivity between the GLAD film material and the byproduct of the organosilane attachment can lead to destruction of the film. Use of an alternate organosilane reagent was shown to eliminate this problem. The combination of morphological and chemical tunability of our nanostructured materials will lead to an exceptional level of control over surface properties and will allow us to engineer these materials for future applications such as optical filters and chemical sensors.

Acknowledgment. The authors gratefully acknowledge the Natural Sciences and Engineering Research Council of Canada for financial support, G. Gelves and Professor J. Haber (Chemistry) for assistance with electrochemistry experiments, G. D. Braybrook for the SEM imaging, the staff of the University of Alberta NanoFab for their assistance, and D. Karpuzov and the Alberta Centre for Surface Engineering and Sciences for the surface science characterization.

CM061709T